Available online at www.sciencedirect.com
SciVerse ScienceDirect
Scripta Materialia 67 (2012) 911–914
Scripta MATERIALIA
www.elsevier.com/locate/scriptamat

# Atomic-scale processes revealing dynamic twin boundary strengthening mechanisms in face-centered cubic materials

Z.Q. Yang,[a,b,*] M.F. Chisholm,[b] L.L. He,[a] S.J. Pennycook[b] and H.Q. Ye[a]

[a]*Shenyang National Laboratory for Materials Science, Institute of Metal Research, Chinese Academy of Sciences, Shenyang 110016, China*

[b]*Division of Materials Science and Technology, Oak Ridge National Laboratory, Oak Ridge, TN 37831, USA*

Received 16 July 2012; revised 28 August 2012; accepted 28 August 2012
Available online 1 September 2012

We report experimental investigations on interactions/reactions between dislocations and twin boundaries in Al. The absorption of screw dislocations via cross-slip and the production of stair-rods via reactions with non-screw dislocations were verified by atomic resolution imaging. Importantly, the resulting partial dislocations moving along twin boundaries can produce secondary sessile defects. These immobile defects act as obstacles to other dislocations and also serve to pin the twin boundaries. These findings show the atomic-level dynamics of the dislocation–twin boundary processes and the unique strengthening mechanism of twin boundaries in face-centered cubic metals.
© 2012 Acta Materialia Inc. Published by Elsevier Ltd. All rights reserved.

*Keywords:* Twin boundary; Dislocation; Strengthening; Plasticity; Face-centered cubic metals

Dislocations and internal boundaries are two fundamental elements underpinning the strength and ductility of metals [1–4]. The Hall–Petch relationship describes the grain size effect on the strength of the material, assuming that internal boundaries act as mechanically static obstacles to dislocation motion [5,6]. However, the dynamic atomic-level response of dislocations and internal boundaries is less well understood, although grain boundaries (GBs) are generally known to emit and/or annihilate dislocations during plastic deformation [2,7]. While twin boundaries (TBs) are coherent planar defects, they are found to influence the mechanical behavior of many materials [8–17]. Deformation twins are believed to play critical roles in the high strength and ductility of austenitic steels with a high work hardening rate [13]. A large fraction of TBs is important in superalloys that are used for very high temperature applications [14]. Strengthening materials by conventional grain refinement (introducing more GBs) invariably affects ductility adversely. Interestingly, TBs are found to strengthen metals without severe loss of ductility [15–17]. Additionally, materials containing a high density of pre-existing TBs or dynamic deformation twins show higher work hardening rates [9]. This indicates that these twins, in addition to acting as simple static barriers, must also interact with dislocations in other ways. The underlying mechanisms of these additional interactions are still not well understood because of difficulties in obtaining experimental atomic-level data of the actual dislocation–TB interactions. Instead, computer simulations have been performed, elucidating some dislocation–TB interactions/reactions at the atomic level, such as cross-slip of screw dislocation and the formation of Cottrell–Lomer locks [18–23].

Twins in Al are rare due to its high stacking fault (SF) energy [11,20–25]. Deformation twinning has rarely been reported in Al with grains larger than 100 nm, although simulations showed the possibility of deformation twinning in nanocrystalline Al [20]. Reversible twinning was observed once at a crack tip on a thin foil of coarse-grained Al by in situ transmission electron microscopy (TEM) observation [24]. Here, we report experimental observations of dislocation–TB interactions and reactions in Al particles about 100 nm in diameter, providing some significant insights into the unique strengthening mechanism of TBs. Some of the experimental observations have not yet been predicted even by computer simulations. We believe the observed scarcity of twins in these Al particles makes it more

* Corresponding author at: Shenyang National Laboratory for Materials Science, Institute of Metal Research, Chinese Academy of Sciences, Shenyang 110016, China; e-mail: yangzq34@gmail.com

1359-6462/$ - see front matter © 2012 Acta Materialia Inc. Published by Elsevier Ltd. All rights reserved.
http://dx.doi.org/10.1016/j.scriptamat.2012.08.032

straightforward to observe and interpret dislocation–TB interactions. Thus, we used this model system to investigate strengthening mechanisms in face-centered cubic (fcc) metals at the atomic level.

We investigated dislocation–TB interactions and reactions in ultrafine Al particles about 100 nm in diameter by high-resolution TEM (HRTEM). The Al particles were synthesized by evaporation of high-purity (99.995 at.%) aluminum foils. The particles were first passivated, then compacted into disks at 1.0 GPa at room temperature, during which adjacent particles acted as indenters to each other. Microstructures of deformed aluminum particles with twins were investigated in a JEOL 2010 microscope. The amorphous oxide shell encapsulating each Al particle keeps the particles from coalescing and instead forces deformation processes to occur [26].

Figure 1a shows a TEM image of a twinned Al particle about 100 nm in diameter with a dent at the upper right corner. The observed TB is the result of a deformation twin, not a growth twin. A growth twin that could arise from the coalescence of two adjacent particles during consolidation would be expected to contain a symmetrical neck due to the high surface tension at the boundary position. Figure 1b is an HRTEM image of the TB recorded along the $[1\bar{1}0]$ zone axis. Steps going up and down can be identified along the TB in the HRTEM image, indicating that Shockley partial dislocations with different Burgers vectors have moved along this boundary. It can thus be concluded that dislocation–TB reactions must take place in the Al particle. Moreover, dislocations on different $(1\,1\,\bar{1})$ slip planes have reached and reacted with the TB.

Figure 2a is an HRTEM image showing the atomic-scale structures from one local region where dislocation–TB reactions occurred. First, a notch, about 1 nm deep and 3 nm wide, is identified between a pair of steps. The atomic columns at the notch's walls deviate from the ideal $[1\bar{1}0]$ projections of the fcc lattice positions,

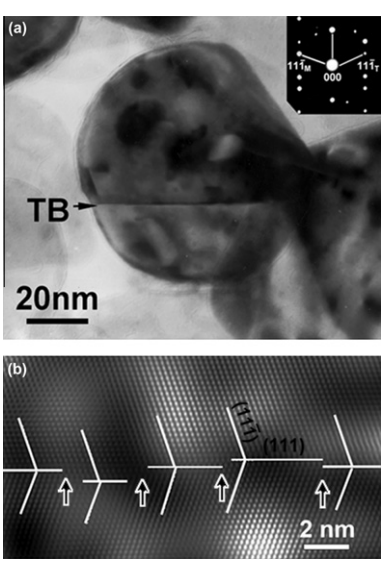


**Figure 1.** A deformed twinned Al particle. (a) TEM image; the inset shows the $[1\bar{1}0]$ electron diffraction pattern. (b) HRTEM image, with the local twin relation indicated.

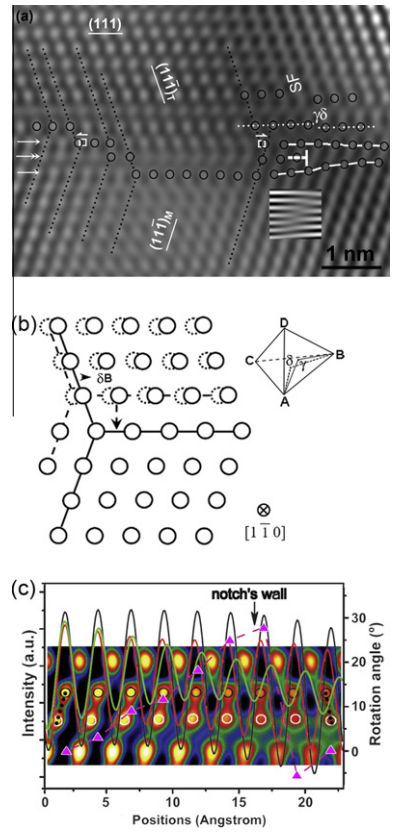


**Figure 2.** Atomic configurations of dislocation–TB reactions. (a) HRTEM image. ○, atomic columns in the TB plane and its vicinity; □, ideal positions of atomic columns; ←, shift direction; ⊥, 60° dislocation; white bars, outline of lattice distortion around the dislocation core. (b) Atomic model showing TB migration with the Thompson's notation. (c) Lattice distortion in the vicinity of the core of a 90° partial, overlapped on the image. The black curve shows the line profile for a reference {1 1 1} plane in the matrix; the red and green curves represent the line profiles for the two planes marked by black and white circles, respectively. . . . and ▲, local $(1\,1\,\bar{1})$ lattices and their rotation angles. (For interpretation of the references to color in this figure legend, the reader is referred to the web version of this article.)

as shown schematically by the shift from the white square to the black circle in Figure 2a. Atomic columns on both walls of the notch in the two (1 1 1) planes marked by arrows deviated from their ideal fcc lattice positions by about one-third of the distance between two neighboring atomic columns, indicating the existence of 30° partial dislocations at the notch's walls. An incident perfect screw dislocation in plane ABD could split into two 30° Shockley partials in the TB plane ABC via cross-slip:

$$\mathrm{AB}_{\mathrm{ABD}} = A\gamma + \gamma\mathrm{B} \xrightarrow{\text{cross-slip}} A\delta + \delta\mathrm{B} = \mathrm{AB}_{\mathrm{ABC}} \quad (1)$$

This reaction is energetically favored, since no cross-slip energy barrier is required once a TB is present [7]. Glide of the dissociated Shockley dislocations moves the TB one atomic layer, as shown in Fig. 2b. TB migration via absorption of dislocations releases some resistance to the motion and multiplication of other dislocations inside the grain by decreasing the dislocation density. This process refreshes the capability of the grain to plastically deform. This might be one of

the reasons why nanotwinned metals [15] have considerable plasticity. In addition, the present observations suggest that deformation twinning in this particle originated from the nucleation of an SF at the top surface (similar to the emission of Shockley partials from GBs in bulk material [16,20]), and subsequent reactions with screw dislocations that moved the boundary to the center of the particle. The dislocation at the left side of the notch in the double-arrowed (1 1 1) plane in Fig. 2a is a 90° partial from dissociation of a 60° dislocation **CA** or **CB** gliding originally along the TB plane ABC, and the lattice distortion is quantified in Fig. 2c. The local lattice spacing in the two circle-marked planes is compressed (black circles, red curve) and expanded (white circles, green curve), respectively, compared with the reference lattice (black curve), as shown by the corresponding line profiles for each plane. The local $(1\,1\,\bar{1})$ lattices rotate gradually from the ideal fcc lattice in the lower grain to that in the upper twin across the notch's wall, which matches the Burgers vector of a 90° partial. The lattice distortion along the TB is expected to create a repulsive stress field to oppose dislocation motion towards the TB, strengthening the material. Additionally, the existing partials can form pile-ups along the TB [20,23], providing a back stress to subsequent dislocation–TB reactions. This would then require an increased applied load to push the lattice dislocations into the TB.

Also shown in Figure 2a is the existence of a stair-rod dislocation, **γδ**, as evidenced by the identified misfit of (1 1 1) planes. This dislocation results from a reaction between a 60° perfect dislocation and the TB, as:

$$\mathrm{DA} \rightarrow D\gamma + \gamma\mathrm{A} \rightarrow D\gamma + \gamma\delta + \delta\mathrm{A} \qquad (2)$$

in which the leading partial, **γA**, is further dissociated into a 30° partial, **δA** on the TB plane and the stair-rod dislocation, **γδ** (1/6 [1 1 0]). The trailing partial, **Dγ**, the stair-rod, **γδ**, and the SF in between formed a Cottrell–Lomer lock [7], while the 30° partial **δA** glided away on the original TB. The resulting stair-rod dislocation makes it more difficult for subsequent dislocations to glide along the TB.

A 60° perfect dislocation arriving at the TB was observed below the stair-rod, **γδ**, in the lower grain, as shown by "⊥" in Fig. 2a (the inset shows the corresponding Fourier-filtered image). According to the lattice distortion indicated by the white bars, the strain field of this incident 60° dislocation clearly indicates strong repulsion from the TB. It is not obvious if this repulsion is primarily due to the presence of the TB or the stair-rod dislocation.

Figure 3a is an HRTEM image showing two partials coming together on the same side of the TB. The left and right dislocations are respectively $\mathbf{b_1} = 1/6\ [\bar{2}\,1\,1]$ and $\mathbf{b_2} = 1/6\ [1\,\bar{2}\,1]$ partials, which advance the TB by shifting atoms originally on lattice sites "*A*" to "*B*", as shown in Figure 3b. The atoms in between the two partials were thus subjected to stresses forcing them to move from sites "*A*" to positions just above the occupied "*C*" sites in the plane underneath. However, if the two partials react, they would produce another partial dislocation that is not permissible. $1/6[\bar{2}\,1\,1] + 1/6[1\,\bar{2}\,1] = 1/6\ [\bar{1}\,\bar{1}\,2] = -\mathbf{b}_3$ is not a permissible glide direction on the original TB [7]. Figure 3c shows the $[1\,\bar{1}\,0]$ projection

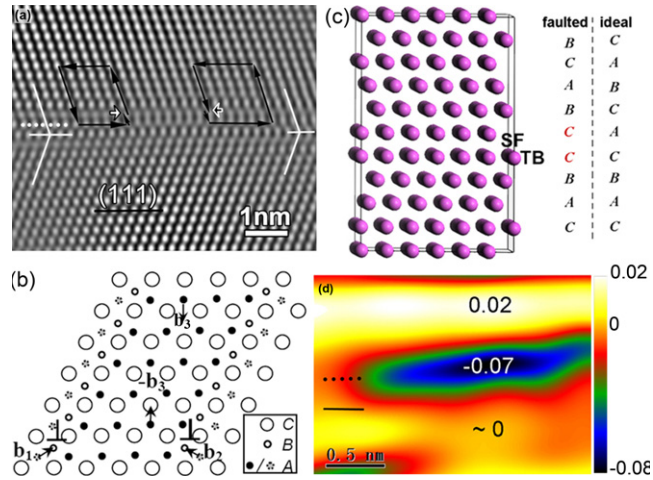


**Figure 3.** Meeting of two partials on the same (1 1 1) plane. (a) HRTEM image. Burgers circuits are outlined by black arrows. (b and c) atomic model for an abnormal stacking adjacent to the TB viewed along $[1\,\bar{1}\,0]$ and [1 1 1], respectively. In (b), the atoms originally at the dotted circles were shifted to the open circles via glide, as indicated by the Burgers vectors $\mathbf{b_1}$ and $\mathbf{b_2}$, and the "⊥" symbols indicate the corresponding partials. In (c), the abnormal and normal stacking sequences are given. (d) Strain map surrounding the abnormal SF. Horizontal solid and dotted lines (a and d) mark the new and original TBs, respectively. (For interpretation of the references to color in this figure legend, the reader is referred to the web version of this article.)

for the unexpected stacking seen between the two dislocations in Figure 3a. Figure 3d shows the strain surrounding the defects, with a maximum lattice contraction about 7% perpendicular to the fault plane rather than expansion that is expected ("*C–C*" stacking is less close-packed than "*A–C*"). The observed lattice contraction suggests that vacancies are present between the dislocations. The lattice contraction observed here is not present at SFs produced by ball-milling and/or a Frank loop induced by electron beam irradiation in Al [20,24].

Figure 4a is an HRTEM image showing the interaction of two 30° partials gliding on two different (1 1 1) slip planes. The left partial "1" (1/6 $[\bar{1}\,2\,\bar{1}]$) originates from the dissociation of a dislocation in the lower grain and the right partial "2" (1/6 $[2\,\bar{1}\,\bar{1}]$) is from the upper twin, as depicted in Figure 4b. Partial "1" glides on the plane above the original TB plane and moves the TB one atomic layer up, while glide of partial "2" advances the TB one atomic layer down. Further glide of partial "1" past the point where the two partials are vertically aligned would bring about an SF requiring higher stress to move the dislocation. More importantly, the 1/6 $[2\,\bar{1}\,\bar{1}]$ glide of partial "2" is not permitted in the lower grain after the 1/6 $[\bar{1}\,2\,\bar{1}]$ detwinning by partial "1", since it would produce a local "*B–B*" stacking, as shown schematically in Figure 4b. Therefore, the two partials obstruct each other. The defect structures resulting from the dislocation–TB reactions shown in Figures 3 and 4 make the TB migration difficult, and also increase the strengthening effect of the TB. The complex defect structures we observed resulted from multiple dislocation–TB reactions. These defect structures have not been predicted by simulations, since simulations usually

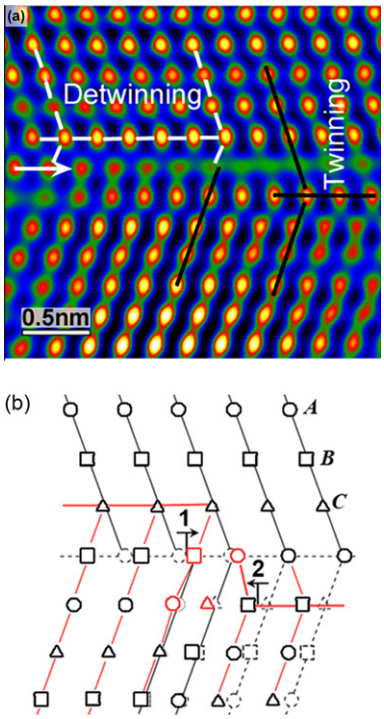


**Figure 4.** Meeting of two partials on two consecutive (1 1 1) planes. (a) HRTEM image. (b) Atomic model. The white arrow in (a) and the horizontal dashed line in (b) indicate the original TB plane. In (b), the moving direction of partials is indicated by arrows, while the dashed $(1\,1\,\bar{1}_M)$ planes represent those before the dislocation–TB reaction. (For interpretation of the references to color in this figure legend, the reader is referred to the web version of this article.)

model single event dislocation–TB interactions [27]. For the real Al nanoparticles under compression, each particle was contacted by surrounding particles along various directions, which resulted in complex dislocation activities inside the grain.

It was demonstrated that even energetically unfavorable dissociation reactions could occur for leading/twinning Shockley partials impinging TBs in materials with relatively low SF energies [28]. Twin–twin interaction was also often observed in materials with low SF energies [28,29], which might be rare in materials with high SF energies. Therefore, the effect of TBs on the strain hardening behaviors could be slightly different for materials with different SF energies.

Using plastically deformed Al particles, our atomic-scale observations reveal how TBs can impede dislocation motion. The TBs facilitate plasticity by absorbing screw dislocations. In addition, the TBs impede dislocation motion by producing sessile defects via the following processes: (i) formation of stair-rods and/or Cottrell–Lomer locks directly via reactions with non-screw incident dislocations; and (ii) production of sessile defects on the TB plane that arise from reactions between dissociated partials moving along the TBs. The observed active participation of the TBs in dislocation reactions has important ramifications on the strengthening mechanisms in fcc materials.

We thank H. Cong for sample preparation. This work was supported by the NSFC (51171189), the MoST of China (2009BC623705) and Liaoning Province. Z.Q.Y., M.F.C. and S.J.P. are supported by Office of Basic Energy Sciences, Materials Sciences and Engineering Division of the US Department of Energy.

[1] F.F. Csikor, C. Motz, D. Weygand, M. Zaiser, S. Zapperi, Science 318 (2007) 251.
[2] J.P. Hirth, R.C. Pond, J. Lothe, Acta Mater. 55 (2007) 5428.
[3] B. Devincre, T. Hoc, L. Kubin, Science 320 (2008) 1745.
[4] V.V. Bulatov, L.L. Hsiung, M. Tang, Nature 440 (2006) 1174.
[5] E.O. Hall, Proc. Phys. Soc. London B 64 (1951) 747.
[6] N.J. Petch, J. Iron Steel Inst. 174 (1953) 25.
[7] J.P. Hirth, J. Lothe, Theory of Dislocations, John Wiley & Sons, New York, 1982.
[8] L. Lu, X. Chen, X. Huang, K. Lu, Science 323 (2009) 607.
[9] Q. Yu, Z.W. Shan, J. Li, X.X. Huang, L. Xiao, J. Sun, E. Ma, Nature 463 (2010) 335.
[10] N. Stanford, U. Carlson, M.R. Barneet, Metall. Mater. Trans. A 39 (2008) 934.
[11] M.W. Chen, E. Ma, K.J. Hemker, H.W. Sheng, Y.M. Wang, X.M. Cheng, Science 300 (2003) 1275.
[12] Z.Q. Yang, M.F. Chisholm, B. Yang, X.L. Ma, Y.J. Wang, M.J. Zhuo, S.J. Pennycook, Acta Mater. 60 (2012) 2637.
[13] X.Y. Li, Y.J. Wei, L. Lu, K. Lu, H.J. Gao, Nature 464 (2010) 877.
[14] Z.X. Wu, Y.W. Zhang, D. Srolovitz, Acta Mater. 57 (2009) 4508.
[15] J. Li, K.J. Van Vliet, T. Zhu, S. Yip, S. Suresh, Nature 418 (2002) 307.
[16] J. Schiøtz, K.W. Jacobsen, Science 301 (2003) 1357.
[17] V. Yamakov, D. Wolf, S.R. Phillpot, A.K. Mukherjee, H. Gleiter, Nature Mater. 1 (2002) 1.
[18] V. Yamakov, D. Wolf, S.R. Phillpot, H. Gleiter, Acta Mater. 50 (2002) 5005.
[19] V. Yamakov, D. Wolf, S.R. Phillpot, H. Gleiter, Acta Mater. 51 (2003) 4135.
[20] M.P. Dewald, W.A. Curtin, Phil. Mag. 87 (2007) 4615.
[21] X.Z. Liao, F. Zhou, E.J. Lavernia, D.W. He, Y.T. Zhu, Appl. Phys. Lett. 83 (2003) 5062.
[22] Y.T. Zhu, X.Z. Liao, S.G. Srinivasan, Y.H. Zhao, M.I. Baskes, F. Zhou, E.J. Lavernia, Appl. Phys. Lett. 85 (2004) 5049.
[23] B.Q. Li, M.L. Sui, B. Li, E. Ma, S.X. Mao, Phys. Rev. Lett. 102 (2009) 205504.
[24] K. Hashihara, F. Inoko, Acta Mater. 49 (2001) 3051.
[25] T.C. Lee, I.M. Robterson, H.K. Birnbaum, Phil. Mag. A 62 (1990) 131.
[26] Z.Q. Yang, J. Chen, L.L. He, H.T. Cong, H.Q. Ye, Acta Mater. 57 (2009) 3633.
[27] Z.H. Jin, P. Gumbsch, K. Albe, E. Ma, K. Lu, H. Gleiter, Acta Mater. 56 (2008) 1126.
[28] L. Remy, Matall. Trans. A 12 (1981) 387.
[29] S. Mahajan, G.Y. Chin, Acat Metall. 21 (1973) 173.